Acta Crystallographica Section F
Structural Biology and Crystallization Communications
ISSN 1744-3091

Purification, crystallization and preliminary X-ray crystallographic analysis of *Arabidopsis thaliana* dynamin-related protein 1A GTPase-GED fusion protein

Xiaoyue Chen,[a]‡ Xuanhao Xu,[b]‡ Yuna Sun,[c] Jingwen Zhou,[d] Yuanyuan Ma,[e] Liming Yan[a]* and Zhiyong Lou[a]*

[a]Laboratory of Structural Biology and MOE Laboratory of Protein Science, School of Medicine, Tsinghua University, Beijing 100084, People's Republic of China, [b]College of Life Science, China Agricultural University, Beijing 100084, People's Republic of China, [c]National Laboratory of Macromolecules, Institute of Biophysics, Chinese Academy of Science, Beijing 100101, People's Republic of China, [d]Beijing No. 8 Middle School, Beijing, People's Republic of China, and [e]College of Life Science, Nankai University, Tianjin 300071, People's Republic of China

‡ These authors contributed equally.

Correspondence e-mail: yanlm@xtal.tsinghua.edu.cn, louzy@xtal.tsinghua.edu.cn

Received 20 September 2011
Accepted 10 November 2011

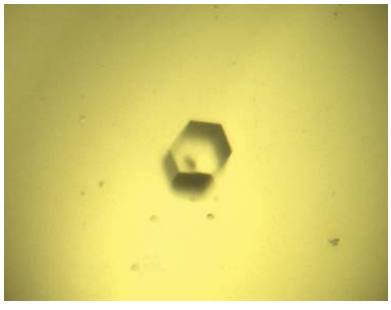

Plant-specific dynamin-related proteins play crucial roles in cell-plate formation, endocytosis or exocytosis, protein sorting to the vacuole and plasma membrane and the division of mitochondria and chloroplasts. In order to determine the crystal structure and thus to obtain a better understanding of the biological functions and mechanisms of dynamin-related proteins in plant cells, the GTPase domain of *Arabidopsis thaliana* dynamin-related protein 1A (*At*DRP1A) fused to its GTPase effector domain (GED) was crystallized in a nucleotide-associated form using polyethylene glycol 3350 as precipitant. The hexagonal crystals (space group $P6_1$) had unit-cell parameters $a = b = 146.2$, $c = 204.3$ Å, and diffraction data were collected to 3.6 Å resolution using synchrotron radiation. Four molecules, comprising two functional dimers, are assumed per asymmetric unit, corresponding to a Matthews coefficient of 3.9 Å^3 Da^{-1} according to the molecular weight of 39 kDa.

1. Introduction

Dynamins and dynamin-related proteins (DRPs) constitute a large superfamily of GTPases that are found in animals, plants and bacteria (Praefcke & McMahon, 2004). They play essential roles in core cellular processes such as endocytosis and clathrin-mediated endocytosis (Damke *et al.*, 1994), post-trans-Golgi network trafficking (Nicoziani *et al.*, 2000), mitochondrial fusion and fission (Herlan *et al.*, 2003), peroxisome fission (Koch *et al.*, 2003), chloroplast morphology (Gao *et al.*, 2006), actin dynamics (Schafer *et al.*, 2002) and pathogen resistance (Praefcke & McMahon, 2004; Chen *et al.*, 2011). Their key features, which include large molecular size, high basal GTP hydrolysis and self-assembly into filamentous helices, distinguish members of the dynamin family from other classical signalling and regulatory GTPases (Praefcke & McMahon, 2004; Xue *et al.*, 2011). Dynamins and other structurally related family members primarily consist of a GTPase domain, a middle domain and a GTPase effector domain (GED) which regulates and responds to hydrolysis of the GTPase domain (Hong *et al.*, 2003; Gout *et al.*, 1993). The GED and the N- and C-termini of the GTPase domain form a so-called three-helical bundle signalling element (BSE) that regulates dynamin function (Chappie *et al.*, 2009, 2010).

Currently, six dynamin-related subfamilies (with 16 members in *Arabidopsis thaliana*), named DRP1–6, have been identified in plants based on their predicted domain structures, amino-acid conservation and functional analyses (Bednarek & Backues, 2010; Hong *et al.*, 2003). Among these plant DRPs, the members of the DRP1 subfamily are referred to as the 'plant-specific dynamins' (Hong *et al.*, 2003). Currently, five of the 16 DRP members found in *A. thaliana*, with similar molecular sizes ranging from 610 to 621 amino-acid residues, are grouped into the *Arabidopsis* DRP1 subfamily and are named *At*DRP1A–*At*DRP1E. Although they share over 80% primary sequence identity, the high variability in their tissue-distribution profiles (Schmid *et al.*, 2005) suggests that they play distinct biological roles in plant cells (Hong *et al.*, 2003). *At*DRP1A is localized to the cytoplasmic surface of the plasma membrane to form cell plates in cytokinetic cells (Hong *et al.*, 2003; Kang *et al.*, 2001; Gu & Verma,

1997) and *At*DRP1A may also play specific roles in the plasma membrane (Kang *et al.*, 2003) and cytoskeleton (Hong *et al.*, 2003). In addition, *At*DRP1A has been shown to interact with *At*DRP2B (Fujimoto *et al.*, 2008) and to form a complex which regulates not only the fission of the neck of the clathrin-coated pit (CCP) but also the maturation of the CCP during endocytosis in *Arabidopsis* cells (Fujimoto *et al.*, 2010; Huang *et al.*, 2010). Moreover, *At*DRP1A has been shown to associate with PIN-FORMED (PIN) proteins, which are restricted to the cell plate, to play an essential role in the establishment of cell polarity in a very recent report (Mravec *et al.*, 2011). However, the structure and mechanisms of *At*DRP1A are poorly understood. In order to obtain functional and structural insights into plant-specific DRPs, we have engineered a GTPase-GED fusion protein from *At*DRP1A (hereafter termed *At*DRP1A GG); here, we report the purification, crystallization and preliminary crystallographic studies of *At*DRP1A GG.

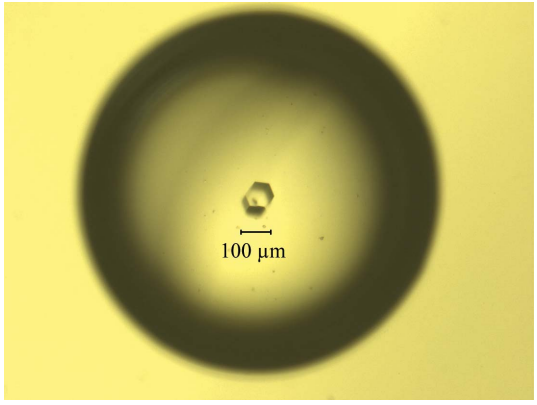

Figure 1
A single crystal of *At*DRP1A GG in a hexagonal crystal form.

2. Protein expression and purification

The coding sequence for *At*DRP1A was amplified by PCR from a in-house *A. thaliana* cDNA library. Four primers, 5′-CGCGGATCCA-TGGAAAATCTGATCTCTCTG-3′, 5′-CCGCTCGAGTCACCAA-TCCGAGATCGATGCTGTT-3′, 5′-CATGGTACTGACAGCCGG-GTCGATCCAGCAATCATGGAGAGA-3′ and 5′-GACCCGGC-TGTCAGTACCATGTGCAATAGGCTTTCCAAGGCGA-3′, were designed and used to generate an *At*DRP1A fusion protein consisting of residues 1–316 of the GTPase domain and residues 585–606 of GED fused by a flexible linker with the primary sequence HGTD-SRV as suggested from human dynamin (Chappie *et al.*, 2009). The PCR conditions were as follows: 30 cycles of 1 min at 367 K, 1 min at 328 K and 2 min at 345 K. The purified PCR products were digested with *Bam*HI and *Xho*I and then inserted into the expression vector pGEX-6p-1 (GE Healthcare) with the same digested sites. After transformation into *Escherichia coli* DH5α, the cloned fragments were completely sequenced (Zhou *et al.*, 2010). The recombinant plasmid was transformed into *E. coli* BL21 (DE3).

The transformed cells were cultured at 310 K in LB medium containing 100 mg l^{-1} ampicillin. When the OD_{600} reached 0.8, the culture was cooled to 289 K and induced with 0.5 m*M* isopropyl β-D-1-thiogalactopyranoside (IPTG). After overnight induction, the cells were harvested by centrifugation at 5000*g* for 10 min at 277 K. The

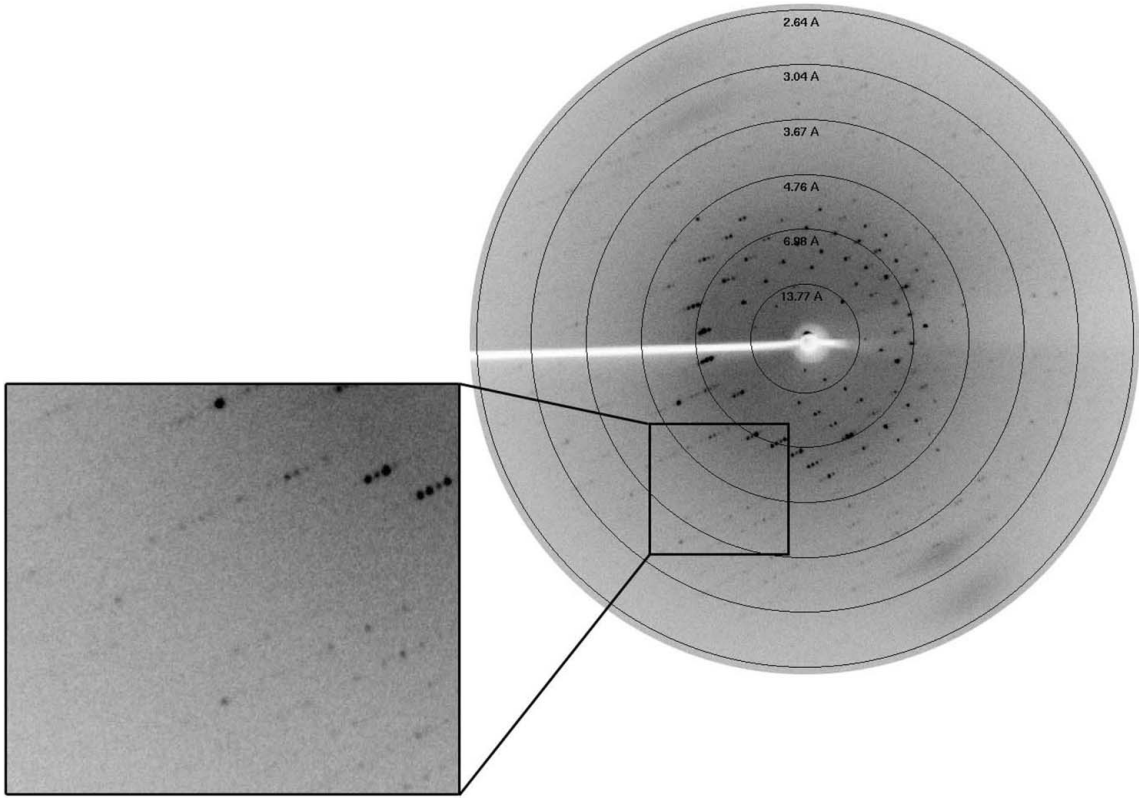

Figure 2
A typical diffraction pattern of an *At*DRP1A GG crystal. The exposure time was 5 s, the crystal-to-detector distance was 200 mm and the oscillation range per frame was 0.5°. The diffraction image was collected on a MAR 165 CCD detector.

cell pellets were resuspended in lysis buffer consisting of 20 m*M* Tris–HCl pH 8.0, 150 m*M* NaCl and disrupted using an ultrahigh-pressure cell disrupter (JNBIO, Guangzhou, People's Republic of China) at 277 K. The cell debris was removed by centrifugation at 20 000*g* for 30 min at 277 K. The GST-tagged protein was purified by GST-glutathione affinity chromatography, cleaved with PreScission protease (GE Healthcare) and eluted with a buffer consisting of 20 m*M* Tris pH 8.0, 150 m*M* NaCl. Purified monomeric *At*DRP1A GG sample was concentrated in a buffer consisting of 20 m*M* Tris–HCl pH 8.0, 150 m*M* NaCl, 2 m*M* EGTA, 4 m*M* $MgCl_2$, 1 m*M* DTT. The yield of *At*DRP1A GG was 2–3 mg per litre of bacterial culture.

Previous studies have shown that the interaction between the GTPase domain and the GED domain is important for regulating dynamin function. To generate *At*DRP1A GG dimers, the sample was further incubated for 30 min at 310 K with 2 m*M* GDP, 1.5 m*M* $AlCl_3$ and 15 m*M* NaF to produce the transition-state mimic AlF_4^-. The *At*DRP1A GG solution was then loaded onto a Superdex 200 column (GE Healthcare) to isolate dimeric fractions.

3. Crystallization

Freshly prepared dimeric *At*DRP1A GG samples were concentrated to 5 mg ml^{-1} in a buffer consisting of 20 m*M* Tris–HCl pH 8.0, 150 m*M* NaCl. Screening for initial crystallization conditions was performed by the hanging-drop vapour-diffusion method using commercially available crystal screening kits from Hampton Research (Crystal Screen, Crystal Screen 2, PEG/Ion and SaltRx) at 291 K. Droplets consisting of 1 µl protein solution (5 mg ml^{-1}) and 1 µl reservoir solution were equilibrated against 500 µl reservoir solution in 24-well plates.

After 3 d, hexagonal prism-shaped crystals of various sizes were observed under five conditions from Crystal Screen and PEG/Ion. Most of these initial crystals showed only limited diffraction. Further crystallization optimization was performed by carefully adjusting the concentration of precipitant and buffer pH together with the protein concentration in 120 droplets. Eventually, a condition consisting of 160 m*M* sodium formate, 16%(*w*/*v*) polyethylene glycol 3350, 40 m*M* magnesium chloride, 6%(*w*/*v*) 2-propanol, 20 m*M* HEPES pH 7.5 was found to produce large single crystals with dimensions of 100 × 100 × 300 µm (Fig. 1) within 2 d. However, these well shaped crystals still diffracted poorly and most of them only showed diffraction to 4.5 Å resolution. Large numbers (over 100) of these crystals were carefully screened to find a crystal with better diffraction.

4. X-ray diffraction analysis

The *At*DRP1A GG crystals were transferred into mother-liquor solution supplemented with 15%(*v*/*v*) glycerol, placed directly into a nylon loop and cooled in a cold nitrogen stream at 100 K. X-ray diffraction data were collected on beamline 1W2 of Beijing Synchrotron Radiation Facility (BSRF) at a wavelength of 1.0000 Å using a MAR 165 CCD detector. The crystal belonged to space group $P6_1$, with unit-cell parameters $a = b = 146.2$, $c = 204.3$ Å (Fig. 2). The raw data were processed with the *HKL*-2000 program suite (Otwinowski & Minor, 1997).

Molecular replacement was performed using the crystal structure of the human dynamin GG dimer (PDB entry 2x2e; Chappie *et al.*, 2010), which shares 35% sequence identity with *At*DRP1A, as the initial search model. This procedure was performed using *Phaser* (McCoy *et al.*, 2007), but no obvious and correct solution was found according to the rotation and translation functions (*Z* scores of <4).

Table 1
Data-collection and refinement statistics.

Values in parentheses are for the highest resolution shell.

Unit-cell parameters	
$a = b$ (Å)	146.2
c (Å)	204.3
$\alpha = \beta$ (°)	90.0
γ (°)	120.0
Space group	$P6_1$
Wavelength (Å)	1.0000
Resolution (Å)	50.00–3.60 (3.66–3.60)
Total No. of reflections	218698 (10900)
No. of unique reflections	28872 (1454)
Completeness (%)	100.0 (100.0)
Average $I/\sigma(I)$	6.2 (3.4)
R_{merge}† (%)	14.4 (44.8)

† $R_{merge} = \sum_{hkl}\sum_i |I_i(hkl) - \langle I(hkl)\rangle| / \sum_{hkl}\sum_i I_i(hkl)$, where $\langle I(hkl)\rangle$ is the mean of the observations $I_i(hkl)$ of reflection *hkl*.

As the GED is often found in variable conformations in dynamin-family members, this is not surprising. A modified model which consisted of the GTPase domain of human dynamin alone was subsequently used to find the correct molecular-replacement solution and gave clear rotation (rotation *Z* score = 6.5) and translation (translation *Z* score = 9.6) function pairs for four monomers (two functional dimers). Assuming that there are four molecules per asymmetric unit, this gives a Matthews coefficient of 3.9 Å^3 Da^{-1} with a solvent content of 40.6% (Matthews, 1968) considering the molecular weight of 39 kDa. Clear electron density for the GED could also be observed. Further structure refinement and manual building of GED is currently under way. The final statistics for data collection and processing are summarized in Table 1.

All crystallization work was performed in the Structure Biology Laboratory at Tsinghua University. This work was supported by the National Natural Science Foundation of China (grant Nos. 31100208 and 31000332), the Ministry of Science and Technology 973 Project and the National Major Project.

References

Bednarek, S. Y. & Backues, S. K. (2010). *Biochem. Soc. Trans.* **38**, 797–806.
Chappie, J. S., Acharya, S., Leonard, M., Schmid, S. L. & Dyda, F. (2010). *Nature (London)*, **465**, 435–440.
Chappie, J. S., Acharya, S., Liu, Y.-W., Leonard, M., Pucadyil, T. J. & Schmid, S. L. (2009). *Mol. Biol. Cell*, **20**, 3561–3571.
Chen, Q., Wang, Q., Xiong, L. & Lou, Z. (2011). *Protein Cell*, **2**, 55–63.
Damke, H., Baba, T., Warnock, D. E. & Schmid, S. L. (1994). *J. Cell Biol.* **127**, 915–934.
Fujimoto, M., Arimura, S., Nakazono, M. & Tsutsumi, N. (2008). *Plant Cell Rep.* **27**, 1581–1586.
Fujimoto, M., Arimura, S., Ueda, T., Takanashi, H., Hayashi, Y., Nakano, A. & Tsutsumi, N. (2010). *Proc. Natl Acad. Sci. USA*, **107**, 6094–6099.
Gao, H., Sage, T. L. & Osteryoung, K. W. (2006). *Proc. Natl Acad. Sci. USA*, **103**, 6759–6764.
Gout, I., Dhand, R., Hiles, I. D., Fry, M. J., Panayotou, G., Das, P., Truong, O., Totty, N. F., Hsuan, J., Booker, G. W., Campbell, I. D. & Waterfield, M. D. (1993). *Cell*, **75**, 25–36.
Gu, X. & Verma, D. P. (1997). *Plant Cell*, **9**, 157–169.
Herlan, M., Vogel, F., Bornhovd, C., Neupert, W. & Reichert, A. S. (2003). *J. Biol. Chem.* **278**, 27781–27788.
Hong, Z., Bednarek, S. Y., Blumwald, E., Hwang, I., Jurgens, G., Menzel, D., Osteryoung, K. W., Raikhel, N. V., Shinozaki, K., Tsutsumi, N. & Verma, D. P. (2003). *Plant Mol. Biol.* **53**, 261–265.
Huang, X., Song, X. & Zhu, P. (2010). *Acta Biophys. Sin.* **26**, 570–578.
Kang, B.-H., Busse, J. S. & Bednarek, S. Y. (2003). *Plant Cell*, **15**, 899–913.
Kang, B.-H., Busse, J. S., Dickey, C., Rancour, D. M. & Bednarek, S. Y. (2001). *Plant Physiol.* **126**, 47–68.

Koch, A., Thiemann, M., Grabenbauer, M., Yoon, Y., McNiven, M. A. & Schrader, M. (2003). *J. Biol. Chem.* **278**, 8597–8605.
Matthews, B. W. (1968). *J. Mol. Biol.* **33**, 491–497.
McCoy, A. J., Grosse-Kunstleve, R. W., Adams, P. D., Winn, M. D., Storoni, L. C. & Read, R. J. (2007). *J. Appl. Cryst.* **40**, 658–674.
Mravec, J., Petrášek, J., Li, N., Boeren, S., Karlova, R., Kitakura, S., Pařezová, M., Naramoto, S., Nodzyński, T., Dhonukshe, P., Bednarek, S. Y., Zažimalová, E., de Vries, S. & Friml, J. (2011). *Curr. Biol.* **21**, 1055–1060.
Nicoziani, P., Vilhardt, F., Llorente, A., Hilout, L., Courtoy, P. J., Sandvig, K. & van Deurs, B. (2000). *Mol. Biol. Cell*, **11**, 481–495.
Otwinowski, Z. & Minor, W. (1997). *Methods Enzymol.* **276**, 307–326.
Praefcke, G. J. & McMahon, H. T. (2004). *Nature Rev. Mol. Cell Biol.* **5**, 133–147.
Schafer, D. A., Weed, S. A., Binns, D., Karginov, A. V., Parsons, J. T. & Cooper, J. A. (2002). *Curr. Biol.* **12**, 1852–1857.
Schmid, M., Davison, T. S., Henz, S. R., Pape, U. J., Demar, M., Vingron, M., Schölkopf, B., Weigel, D. & Lohmann, J. U. (2005). *Nature Genet.* **37**, 501–506.
Xue, J. Y., Guan, H. B. & Yan, Q. (2011). *Acta Biophys. Sin.* **27**, 500–506.
Zhou, X., Ren, L., Meng, Q., Li, Y., Yu, Y. & Yu, J. (2010). *Protein Cell*, **1**, 520–536.